2017 21st International Conference on Process Control (PC)
June 6–9, 2017, Štrbské Pleso, Slovakia

Enhancing disturbance rejection performance for the magnitude-optimum-tuned PI controller

Jan Cvejn
Faculty of Electrotechnics and Informatics,
University of Pardubice
Pardubice, Czech Republic
jan.cvejn@upce.cz

***Abstract*—The Magnitude Optimum (MO) tuning method for PI and PID controllers, applied on stable and non-oscillating plants, usually gives fast tracking responses and offers very good process output disturbance-rejection performance, even if the process contains significant dead time. On the other hand, in the cases of plant-input disturbances slow responses may be obtained. The paper deals with this problem for the PI controller case. Enhancing the disturbance-rejection performance is achieved by means of additional filter designed so that the stability margin properties of the MO tuning are preserved.**

Keywords—pid controller; process control; disturbance rejection; magnitude optimum

I. Introduction

The problem of tuning the PID controller for stable linear systems with dead time is of practical importance in process control and still attracts wide interest. The PI version of the PID controller is the most frequently used controller type in the industry [1]. Classical tuning methods [10-12] and other are still popular, but contemporary methods offer enhanced performance, e.g. [9], [2-5]. The dead-time term in the process transfer function can be replaced by its Taylor or Padè approximants. The approximation enables to use methods for systems without dead time for the controller design, but is usually applicable only if the dead-time dynamics is not important. Alternative approaches, based on a compensation of the delay term, such as Smith predictor or Internal model control [1], [7], [8] do not give a controller of the type PI or PID in general.

One relatively simple approach to setting up the PI controller without any approximation of the dead-time dynamics is based on the magnitude optimum (MO) criterion [1-3]. This design criterion requires that the closed loop frequency response magnitude is as flat as possible in the range of low frequencies, i.e.

$$\lim_{\omega\to 0}\left|\frac{L(i\omega)}{1+L(i\omega)}\right| = 1,\ \lim_{\omega\to 0}\frac{d^k}{d\omega^k}\left|\frac{L(i\omega)}{1+L(i\omega)}\right| = 0 \qquad (1)$$

for $k = 1,2,...,k_m$, where $L(i\omega)$ denotes the open-loop frequency response and k_m is as high as possible. The MO-based design is most natural for the reference tracking control tasks, where the closed-loop system should be able to respond quickly to changes of the reference input, or equivalently to efficiently reject disturbances influencing directly the plant output. In this case it usually produces fast non-oscillating responses.

In many situations in process control an exogenous disturbance affects the output indirectly, usually via the plant input. In these cases the MO design sometimes produces rather slow responses. Typically, this situation occurs when the dominant time constant is much larger than the other time constants and τ. In [4,5] a modification of the MO criterion was proposed, which significantly enhances performance in such cases. However, although the plant-input disturbance rejection performance has been improved significantly, the closed-loop stability margin is reduced in comparison to the MO settings in some cases, which may mean more oscillating responses for other kinds of exogenous signals. A similar approach has also been used in [13].

In this paper this problem is approached in a different way, as an alternative to the method mentioned above. Instead of modifying the design criterion, the MO-tuned PI controller is extended with a suitable first-order filter. This extension enables to preserve the stability margin properties of the MO tuning. The PID version of this method with some further enhancements has been proposed in the recent paper [14]. Here, however, the method is presented in a more general form, using characteristic areas for representation of the plant dynamics for low frequencies. The trade-off between tracking performance and disturbance rejection performance in the case of PI or PID controller has been studied recently by more authors, see e.g. [15].

II. The MO tuning of the PI controller

Let us consider stable linear plant with the transfer function

$$F(s) = K\frac{b_n s^n + b_{n-1}s^{n-1} + ... + 1}{a_n s^n + a_{n-1}s^{n-1} + ... + 1}e^{-\tau s} \qquad (2)$$

where $\tau \geq 0$. The controller is considered in the form $R_d(s) = H_R(s)R_0(s)$, where for $\lambda \geq 1$ and $T_d > 0$

$$H_R(s) = \frac{T_d s + \lambda}{T_d s + 1},\ R_0(s) = K_P + \frac{K_I}{s} \qquad (3)$$

Initially, assume $H_R(s)$. The influence of the term $H_R(s)$ is discussed in the next section. To achieve fast setpoint-tracking performance and broad bandwidth, the PI controller $R_0(s)$ can be tuned by means of the MO tuning method. If we write the expansion

$$F(s) = K - A_1 s + A_2 s^2 - A_3 s^3 + ... \tag{4}$$

the coefficients A_k, called characteristic areas, can be computed from the coefficients a_k as follows [2,3]:

$$\begin{aligned} A_1 &= K(a_1 - b_1 + \tau) \\ &... \\ A_k &= K\left((-1)^{k+1}(a_k - b_k) + \sum_{i=1}^{k}(-1)^{k+i}\frac{\tau^i b_{k-i}}{i!}\right) + \\ &+ \sum_{i=1}^{k-1}(-1)^{k+i-1} A_i a_{k-i} \ . \end{aligned} \tag{5}$$

The MO-optimal settings of the controller $R_0(s)$ then can be obtained as

$$\begin{bmatrix} K_I \\ K_P \end{bmatrix} = \begin{bmatrix} -A_1 & K \\ -A_3 & A_2 \end{bmatrix}^{-1} \begin{bmatrix} -0.5 \\ 0 \end{bmatrix}. \tag{6}$$

For non-oscillating processes $F(s)$ without zeros in the transfer function, the MO settings K_I, K_P usually give fast and well damped responses, even for long dead time τ. In these cases the MO settings results in the open-loop Nyquist plot which lies in the half-plane $\{z \mid \operatorname{Re} z \geq -0.5\}$. More specifically, The MO-optimal open-loop Nyquist plot starts at the point $(-0.5, -\infty)$ for $\omega \to 0$ and monotonically tends towards the right half-plane for $\omega < \omega_u$, where ω_u denotes the open-loop ultimate frequency. For a special case of non-oscillating plants this property of the MO settings was analyzed in [6]. It has been experimentally verified that this property is preserved even for moderately oscillating processes. However, for processes with zeros, especially in the left half-plane, settings with reduced stability margin or even non-stabilizing settings are often obtained. Therefore, for plants with zeros the MO method cannot be recommended in general.

III. Enhancing Disturbance Rejection Performance by the Controller Extension

We assume that the plant dynamics is such that MO-optimal open-loop Nyquist plot lies in the half-plane $\{z \mid \operatorname{Re} z \geq -0.5\}$ and for low frequencies monotonically tends towards the right half-plane, as discussed in the previous section. In order to enhance the capability of rejecting the plant-input disturbances, it is possible to increase the low-frequency gain to partially compensate the disturbance lag. This effect can be achieved by means of the term $H_R(s)$ (3).

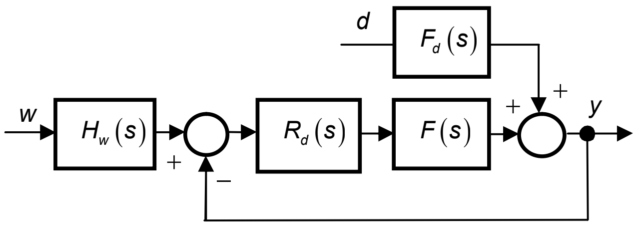

Fig. 1. The control system for disturbance rejection

Consider that the disturbance influences the process output via stable transfer function $F_d(s)$, as shown in Fig. 1, where $H_w(s) = 1$ in the beginning. It is $F_d(s) = F(s)$ in the most common case when the disturbance influences the plant input. Since

$$H_R(s) = \lambda \frac{\lambda^{-1} T_d s + 1}{T_d s + 1} = 1 + \frac{\lambda - 1}{T_d s + 1} \tag{7}$$

in (3), $R_d(i\omega) \approx R_0(i\omega)$ for higher frequencies and the closed-loop response will remain similar to the response for the original MO settings in the higher-frequency band. Note that $\lambda = 1$ corresponds to the original configuration without the filter $H_R(s)$. For low frequencies the parameters λ and T_d can be adjusted to compensate the disturbance dynamics, i.e. to achieve similar disturbance rejection performance as with $F_d(s) = 1$. If we restrict here only to the case $F_d(s) = F(s)$, from (4) it is possible to obtain

$$|F_d(i\omega)|^2 = K^2\left(1 + \frac{A_1^2 - 2KA_2}{K^2}\omega^2 + ...\right). \tag{8}$$

For the special case $F_d(s) = K\exp(-\tau s)/(T_d s + 1)$, where T_d is the filter H_R (3) parameter, we obtain the expansion (4) in the form

$$F_d(s) = K\left(1 - T_d s + T_d^2 s^2 - T_d^3 s^3 + ...\right)e^{-\tau s} \tag{9}$$

and

$$\begin{aligned} |F_d(i\omega)|^2 &= K^2\left(1 - T_d i\omega + T_d^2 (i\omega)^2 + ...\right)\left(1 + T_d i\omega + ...\right) = \\ &= K^2\left(1 - T_d^2\omega^2 + ...\right). \end{aligned} \tag{10}$$

Consequently, if we choose

$$T_d = \frac{1}{K}\sqrt{2KA_2 - A_1^2} \tag{11}$$

(it is assumed that $\left|F_d\left(i\omega\right)\right|^2$ is decreasing, so T_d is real), then

$$\left|F_d(i\omega)\right| \approx |K| / \left|T_d i\omega + 1\right| \tag{12}$$

is a suitable approximation of $\left|F_d(i\omega)\right|$ for low frequencies. If we further consider the model (12), by using (7) it can be written

$$\begin{aligned} \left|G_{yd}\left(i\omega\right)\right| &= \frac{|K|}{\left|T_d i\omega+1\right|}\left|1+\lambda\frac{\lambda^{-1}T_d i\omega+1}{T_d i\omega+1}L_0\left(i\omega\right)\right|^{-1} = \\ &= \frac{|K|}{\left|\lambda^{-1}T_d i\omega+1\right|}\left|1+\frac{T_d\left(1-\lambda^{-1}\right)}{\lambda^{-1}T_d i\omega+1}i\omega+\lambda L_0\left(i\omega\right)\right|^{-1} \end{aligned} \tag{13}$$

where $G_{yd}\left(s\right)$ denotes the transfer function between the disturbance d and the process output y and $L_0\left(i\omega\right)=R_0\left(i\omega\right)F\left(i\omega\right)$. Since $\left|\operatorname{Im}L_0\left(i\omega\right)\right|\to\infty$ for $\omega\to 0$, the term $\left(T_d\lambda^{-1}i\omega+1\right)^{-1}T_d\left(1-\lambda^{-1}\right)i\omega$ in (13) is nearly imaginary and has a negligible influence for $\omega<1/T_d$ and $\lambda>1$. In addition, for very low frequencies $\left|1+\lambda L_0\left(i\omega\right)\right|\approx\lambda\left|1+L_0\left(i\omega\right)\right|$, therefore

$$\left|G_{yd}\left(i\omega\right)\right|\approx\lambda^{-1}\frac{|K|}{\left|\lambda^{-1}T_d i\omega+1\right|}\left|1+L_0\left(i\omega\right)\right|^{-1}. \tag{14}$$

Eq. (14) shows that the disturbance time constant is reduced from T_d to T_d/λ and in comparison with the original response (with the controller $R_0\left(s\right)$), the frequency magnitude response is approximately divided by the factor $\lambda\geq 1$ in the low frequency band. Therefore, it can be expected that the proposed additional filter will substantially increase the disturbance-rejection performance for larger values of λ.

By applying the filter $H_R\left(s\right)$ the open-loop Nyquist plot is no longer close to the line $\left\{z \mid \operatorname{Re}z=-0.5\right\}$ for low frequencies and the stability margin may be reduced for a fixed λ. However, it is possible to adjust the value λ so that the stability margin requirements are fulfilled. Note that it is desirable to choose λ as large as possible to achieve the highest disturbance-rejection performance.

IV. THE COMPUTATION OF λ FOR GIVEN PHASE MARGIN

Let $L_d\left(i\omega\right)=R_d\left(i\omega\right)F\left(i\omega\right)$. To ensure the stability margin, it is possible to use the amplitude margin A_m and the phase margin (PM) requirements [1]. Since $R_d\left(i\omega\right)\approx R_0\left(i\omega\right)$ for higher frequencies and for the considered class of systems the Nyquist plot of $L\left(i\omega\right)$ starts at the point $\left(-0.5,-\infty\right)$ for $\omega\to 0$ and monotonically tends towards the right half-plane for $\omega<\omega_u$, it is possible to assume that $A_m>2$, unless λ is very large. The stability margin in this case seems to be well characterized by the phase margin parameter φ_m, which is defined as the angle $\pi+\angle\left(L_d\left(i\omega_m\right)\right)$, where ω_m is the frequency such that $\left|L_d\left(i\omega_m\right)\right|=1$.

The shape of the MO-optimal Nyquist plot of $L_0\left(i\omega\right)$ is close to the line $\left\{z \mid \operatorname{Re}z=-0.5\right\}$ for $\omega\ll\omega_u$ (Fig. 2). The filter term $H_R\left(s\right)$ moves the Nyquist plot to the left for low frequencies, monotonically with respect to ω. For $\lambda=1$ it is $L_d\left(i\omega\right)=L_0\left(i\omega\right)$ and $\operatorname{Re}L_0\left(i\omega_m\right)\approx-0.5$, which corresponds to $\varphi_m=\pi/3$. For $\varphi_m=\pi/6$ a line going through the origin touches the circle with center at $\left[-1,0\right]$ and radius 0.5 (Fig. 2). This shows that the value of φ_m have to be chosen in the interval $\varphi_m\in\left[30°,60°\right]$ to preserve $\left|L_d\left(i\omega\right)+1\right|\geq 0.5$. The choice $\varphi_m\in\left[40°,45°\right]$ seems to be recommendable in general.

From (7) it follows that

$$L_d\left(i\omega\right)=L_0\left(i\omega\right)+\frac{\lambda-1}{T_d i\omega+1}L_0\left(i\omega\right). \tag{15}$$

Let us define $\omega_c=1/T_d$. If we assume that $\omega_c\ll\omega_m$ (this assumption is discussed later),

$$\frac{\lambda-1}{T_d i\omega_m+1}\approx\frac{\lambda-1}{T_d i\omega_m} \tag{16}$$

holds and consequently

$$\angle L\left(i\omega_m\right)-\angle\left(\frac{\lambda-1}{T_d i\omega_m+1}L\left(i\omega_m\right)\right)\approx\frac{\pi}{2}. \tag{17}$$

From Fig. 2 it can be directly seen that (assuming that (17) holds precisely)

$$\cos\left(\varphi-\varphi_m\right)=-\cos\left(\angle L\left(i\omega_m\right)-\varphi_m\right)=\left|L\left(i\omega_m\right)\right| \tag{18}$$

where $\varphi=\angle L\left(i\omega_m\right)+\pi$. Eq. (18) enables to compute ω_m for chosen φ_m. For known ω_m

$$\lambda=1+T_d\omega_m\tan\left(\varphi-\varphi_m\right) \tag{19}$$

is easily obtained from Fig. 2.

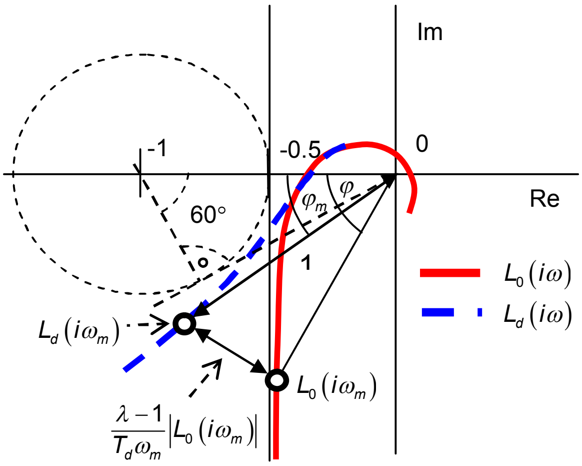

Fig. 2. The determination of λ from the phase margin.

From (18) the frequency ω_m can be easily determined graphically using the plots of $|L_0(i\omega)|$ and $\cos\angle L_0(i\omega)$. Alternatively, it is possible to use iterative computation, based on bisection, see [14] for details. To obtain the settings in analytical form, it is possible to determine ω_m approximately. Since

$$L_0(i\omega)=\frac{K_P i\omega+K_I}{i\omega}\left(K-A_1 i\omega+A_2(i\omega)^2-\ldots\right) \tag{20}$$

for low frequencies, where A_k are given by (5),

$$\begin{aligned}\angle L_0(i\omega) &\approx -\frac{\pi}{2}+\arctan\left(\frac{K_P}{K_I}\omega\right)-\arctan\left(\frac{A_1}{K}\omega\right)\approx \\ &\approx -\frac{\pi}{2}+\left(\frac{K_P}{K_I}-\frac{A_1}{K}\right)\omega\end{aligned} \tag{21}$$

and

$$\begin{aligned}-\cos\left(\angle L_0(i\omega)-\varphi_m\right) &= -\cos\left(\frac{\pi}{2}+\omega\left(\frac{A_1}{K}-\frac{K_P}{K_I}\right)+\varphi_m\right)= \\ &= \sin\left(\omega\left(\frac{A_1}{K}-\frac{K_P}{K_I}\right)+\varphi_m\right)\approx \omega\left(\frac{A_1}{K}-\frac{K_P}{K_I}\right)+\varphi_m .\end{aligned} \tag{22}$$

Further, it is possible to write

$$\begin{aligned}|L_0(i\omega)| &= \sqrt{K_P^2+\left(\frac{K_I}{\omega}\right)^2}\,|F(i\omega)|=\frac{|K_I|}{\omega}P(\omega)|F(i\omega)| \\ P(\omega) &= \sqrt{1+\frac{K_P^2}{K_I^2}\omega^2}\approx 1+\frac{1}{2}\frac{K_P^2}{K_I^2}\omega^2\end{aligned} \tag{23}$$

and from (10) $|F(i\omega)|\approx|K|\left(1-T_d^2\omega^2/2\right)$. It can be easily seen that the closed-loop stability implies $|K||K_I|=KK_I$, so for low ω:

$$|L_0(i\omega)|\approx\frac{KK_I}{\omega}\left(1+\frac{1}{2}\left(\frac{K_P^2}{K_I^2}-T_d^2\right)\omega^2\right). \tag{24}$$

Substituting (22) and (24) into (18) gives the following equation for approximate determination of ω_m:

$$\begin{aligned}&V\omega_m^2+\varphi_m\omega_m=KK_I \\ &V=\left(\frac{A_1}{K}-\frac{K_P}{K_I}\right)-\frac{KK_I}{2}\left(\frac{K_P^2}{K_I^2}-T_d^2\right).\end{aligned} \tag{25}$$

Denote $\omega_+=0.5\left(-\varphi_m+\sqrt{D}\right)/V$, where $D=\varphi_m^2+4VKK_I$, the lowest positive real solution to (25). In tested cases for the basic choice $\varphi_m=\pi/4$ the difference between ω_+ and the precise solution to (18) was always close to 20%. Therefore, using $\omega_m=1.2\,\omega_+$ is recommended, although the multiplication by 1.2 usually has a minor overall effect.

Finally, it is needed to discuss the effect of the approximation (16). The assumption $\omega_c<<\omega_m$, where $\omega_c=1/T_d$, is not fulfilled in general. If $\omega_c<\omega_m$, but the ratio ω_m/ω_c gets close to one, the Nyquist plot corresponding to the approximation of $L_d(i\omega)$ is more curved to the left for low frequencies, while for higher frequencies it is close to the Nyquist plot of $L_d(i\omega)$. If $\omega_m>\omega_c$, the Nyquist plots are closer to each other. Clearly, using the approximation (16) gives similar settings if $\omega_m>\omega_c$ and more conservative settings, i.e. a lower value of λ, if ω_m/ω_c gets close to 1 or is lower. This behavior is desirable, because if $\omega_c\to\omega_m$, the effect of the disturbance lag compensation should be reduced. However, if $\omega_c\geq\omega_m$, it seems to be natural to set $\lambda=1$ and thus to use only the original PI controller without the filter $H_R(s)$. This recommendation is also based on experimental comparisons.

TABLE I. THE CONTROLLER $R_0(s)$ SETTINGS FOR METHODS TESTED IN SECTION VI

	MO		DRMO		ZN	
Plant	K_P	K_I	K_P	K_I	K_P	K_I
$F_1(s)$	1.74	0.172	2.14	0.379	5.92	0.813
$F_2(s)$	5.00	0.50	5.79	2.10	7.36	2.25
$F_3(s)$	0.887	0.087	1.05	0.131	1.58	0.010

TABLE II. THE CONTROLLER EXTENSION FILTER AND THE SETPOINT FILTER PARAMETERS FOR $\varphi_m = 40°$ (THE MO TUNING METHOD ONLY)

Plant	λ	T_d	$\lambda^{-1}T_d$
$F_1(s)$	1.68	10.2	6.10
$F_2(s)$	2.89	10.0	3.46
$F_3(s)$	1.32	10.0	7.57

V. THE SET-POINT FILTERING

If the controller extension is used, the reference tracking response changes as well. If $H_w(s)=1$ is chosen in the scheme in Fig. 1, for the magnitude frequency response between w and y

$$\left|G_{yw}(i\omega)\right| = \left|\frac{H_R(i\omega)L_0(i\omega)}{1+H_R(i\omega)L_0(i\omega)}\right| = \frac{\left|\lambda L_0(i\omega)\right|}{\left|\frac{T_d i\omega+1}{\lambda^{-1}T_d i\omega+1}+\lambda L_0(i\omega)\right|} = \\ = |K|^{-1}\left|\lambda^{-1}T_d i\omega+1\right|\left|G_{yd}(i\omega)\right|\lambda\left|L_0(i\omega)\right| \tag{26}$$

is obtained, where $\left|G_{yd}(i\omega)\right|$ is given by (13). Since $G_{yd}(i\omega)$ has compensated the disturbance lag for low frequencies and the filter $H_R(s)$ effect in addition approximately corresponds to multiplying the disturbance by λ^{-1}, it can be considered that $\lambda\left|G_{yd}(i\omega)\right|$ is similar to $|K|\left|1+L(i\omega)\right|^{-1}$ for low frequencies. This suggests that the factor $\left|\lambda^{-1}T_d i\omega+1\right|$ should be removed from $\left|G_{yw}(i\omega)\right|$ to obtain a similar closed-loop response as without the filter $H_R(s)$. This can be accomplished easily by choosing

$$H_w(s) = \left(\lambda^{-1}T_d s+1\right)^{-1} \tag{27}$$

in the scheme in Fig. 1.

VI. SIMULATION RESULTS

Below, the responses of the closed-loop system in Fig. 1 are shown for the following plants:

$$F_1(s) = \frac{1}{(10s+1)(2s+1)}e^{-s},\ F_2(s) = \frac{1}{10s+1}e^{-s}, \\ F_3(s) = \frac{-2s+1}{(10s+1)(2s+1)}e^{-2s} \tag{28}$$

where the disturbance is considered at the plant input, i.e. $F_{dk}(s) = F_k(s)$, $k = 1...3$. The PI controller $R_0(s)$ settings were obtained from (6). The filter $H_R(s)$ (3) time constant T_d is determined from (11). The parameter λ is computed for the required phase margin $\varphi_m = 40°$ by using the approximate analytical method described in Section IV. The set-point filter $H_w(s)$ settings were computed using (27). Note that for the plant $\exp(-\tau s)/\left((T_1 s+1)...(T_n s+1)\right)$, the expressions (5) yield $A_1 = \tau + \sum_{k=1}^{n} T_k$ and

$$A_2 = -a_2 + \frac{\tau^2}{2} + A_1 a_1 = -\sum_{i\neq j} T_i T_j + \frac{\tau^2}{2} + \left(\sum_{k=1}^{n} T_k\right)^2 + \\ +\tau\sum_{k=1}^{n} T_k = \frac{1}{2}\sum_{k=1}^{n} T_k^2 + \frac{1}{2}\left(\tau + \sum_{k=1}^{n} T_k\right)^2 \tag{29}$$

so $T_d = \left(\sum_{k=1}^{n} T_k^2\right)^{1/2}$. The proposed method is compared with the following tuning methods of the PI controller: the original MO tuning method, the DRMO tuning method [4], based on a modified MO criterion, and the well-known Ziegler-Nichols (ZN) frequency response method [10]. Since the DRMO method was designed to optimize the disturbance rejection properties, the set-point weighting approach [4,1] has been used to decrease overshoots in the reference tracking mode. The controller settings are summarized in Tables 1 and 2.

Figures 3 to 5 show the responses to the unit-step changes of the disturbance signal and the responses to the step-wise reference signal. It is apparent that the proposed tuning method, when compared to the MO settings, results in much better load disturbance rejection performance. The DRMO method gave slightly faster responses, but the stability margin was rather reduced is some cases, which produced more oscillating responses to disturbances influencing the output directly. The ZN method responses are rather oscillatory. The obtained set-point responses are acceptable, but slower than in the case of the original MO configuration.

VII. CONCLUSIONS

Although the MO tuning method of the PI controller for stable and non-oscillating plants usually gives fast closed-loop responses to the set-point signal and provides very good output-disturbance rejection performance, its load-disturbance rejection capabilities are not satisfactory in some cases. The way of removing this problem by means of extending the controller with a first-order filter, plus additional set-point filter, has been proposed. The filter parameters are computed directly from the process time constants, except for a single tuning parameter $\lambda \geq 1$. This parameter was set so that the stability margin characteristic for the MO settings was preserved, based on the required phase margin specification φ_m. For computation of λ a non-iterative analytical method was proposed, which for $\varphi_m = 40°$ gives satisfactory results. The filter settings for $\varphi_m < 40°$ are not recommended, since the responses could contain fast oscillating modes. For $\varphi_m > 45°$ the disturbance rejection performance need not be satisfactory. A lower value of $\lambda > 1$, instead of the computed value, can be used to adjust the balance between tracking and disturbance rejection performance.

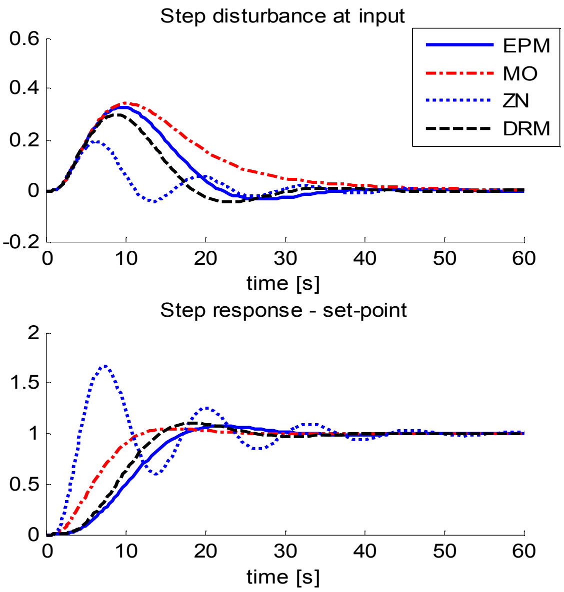

Fig. 3. Plant $F_1(s)$ time responses - the extended controller based on the phase margin specification $\varphi_m = 40°$ (EPM), the original MO settings (MO), the ZN frequency response settings (ZN), the DRMO settings (DRM)

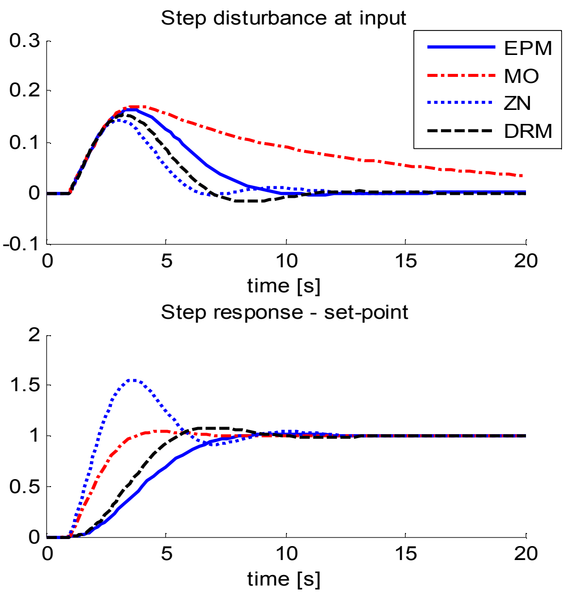

Fig. 4. Plant $F_2(s)$ time responses - the extended controller based on the phase margin specification $\varphi_m = 40°$ (EPM), the original MO settings (MO), the ZN frequency response settings (ZN), the DRMO settings (DRM)

VIII. References

[1] K.J. Åström and T. Hägglund, PID Controllers: Theory, Design, and Tuning, 2nd edition, Instrument Society of America, 1995.

[2] D. Vrančić, Y. Peng, and S. Strmčnik, "A new PID controller tuning method based on multiple integrations", Control Engineering Practice, vol. 7, pp. 623-633, 1999.

[3] D. Vrančić, S. Strmčnik, and D. Juričić, "A magnitude optimum multiple integration tuning method for filtered PID controller", Automatica, vol. 37, pp. 1473-1479, 2001.

[4] D. Vrančić, S. Strmčnik, and J. Kocijan, "Improving disturbance rejection of PI controllers by means of the magnitude optimum method", ISA Transactions, vol. 43, pp. 73-84, 2004.

[5] D. Vrančić, S. Strmčnik, J. Kocijan, and P.B. de M. Oliviera, "Improving disturbance rejection of PID controllers by means of the magnitude optimum method", ISA Transactions, vol. 49, pp. 47–56, 2010.

[6] J. Cvejn, "The design of PID controller for non-oscillating time-delayed plants with guaranteed stability margin based on the modulus optimum criterion", Journal of Process Control, vol. 23, pp. 570-584, 2013.

[7] D.E. Rivera, M. Morari, and S. Skogestad, "Internal model control. 4. PID controller design", Industrial & Engineering Chemistry Process Design and Development, vol. 25, pp. 252–265, 1986.

[8] D. Vrečko, D. Vrančić, D. Juričić, and S. Strmčnik, "A new modified Smith predictor: the concept, design and tuning", ISA Transactions, vol. 0, pp. 1-11, 2000.

[9] Skogestad, S., "Simple analytic rules for model reduction and PID controller tuning". Journal of Process Control 13, pp. 291-309, 2003.

[10] J.G. Ziegler and N.B. Nichols, "Optimum settings for automatic controllers", Transactions of the ASME, vol. 64, pp. 759-768, 1942.

[11] K.L. Chien, J.A. Hrones, J.B. Reswick, "On the automatic control of generalised passive systems", Transactions of the ASME, vol. 52, pp. 175-185, 1952.

[12] G.H. Cohen and G.A. Coon, "Theoretical consideration of retarded control", Transactions of the ASME, vol. 75, pp. 827-834, 1953.

[13] Fišer, J., Zítek, P., and Vyhlídal, T.: "Magnitude optimum design of PID control loop with delay", IFAC-PapersOnLine, vol. 48, pp. 446-451, 2015.

[14] J. Cvejn and D. Vrančić, "The magnitude optimum tuning of the PID controller – improving load disturbance rejection by extending the controller", Transactions of the Institute of Measurement and Control, Prepublished February 1, 2017. DOI 10.1177/0142331216688749.

[15] C. Grimholt and S. Skogestad, "Optimal PI-Control and Verifcation of the SIMC Tuning Rule", IFAC Conf. Advances in PID Control PID'12, Brescia (Italy), 2012.

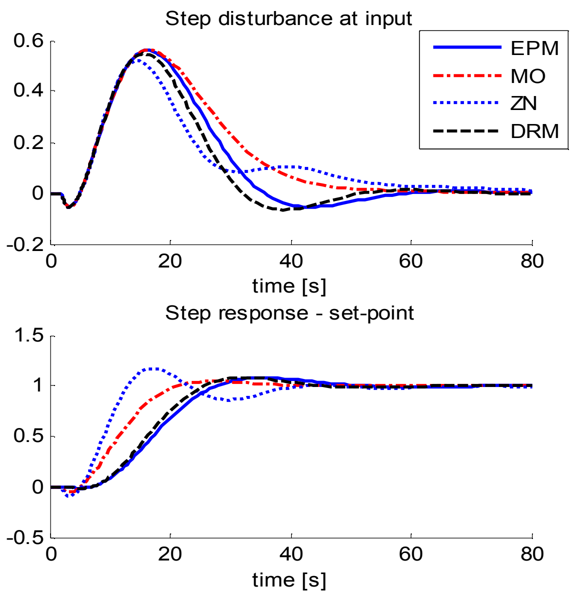

Fig. 5. Plant $F_3(s)$ time responses - the extended controller based on the phase margin specification $\varphi_m = 40°$ (EPM), the original MO settings (MO), the ZN frequency response settings (ZN), the DRMO settings (DRM)